Clin Oral Invest (2010) 14:645–651
DOI 10.1007/s00784-009-0350-9

ORIGINAL ARTICLE

Ex vivo radiographic tooth length measurements with the reference sphere method (RSM)

Felix Roeder · Dan Brüllmann · Bernd d'Hoedt · Ralf Schulze

Received: 24 March 2009 / Accepted: 22 September 2009 / Published online: 15 October 2009

Abstract A reference-based radiographic "reference sphere method" (RSM) for accurate length measurements in (dental) projection radiographs for the assessment of tooth length in dry human mandible sections is evaluated. RSM determines the depth coordinates of reference spheres placed in the object plane from the elliptical distortion of their shadows. Two segments (one canine and one molar) of dry human mandibles were exposed 95 times at different angulations (0–40°) on a dental charge-coupled device receptor. Three steel spheres (diameters d_1=2.00 mm, d_2=3.00 mm) were attached roughly coplanar with the tooth's main axis. Radiographs were assessed once by visual inspection plus manual landmark identification with a mouse-driven cursor. The results were compared to the true tooth length assessed after extraction and to a conventional method (C), i.e., the rule of proportion based on magnification of the sphere shadows. Mean relative length error was 2.28% (d_1) and 0.46% (d_2) for RSM and −13.58% (d_1) and −9.90% (d_2) for C. For both methods, length errors were significantly (p<0.0001) correlated with the inclination relative to the receptor. RSM allows for complete a posteriori determination of the imaging geometry under the assumption of a known source-to-receptor distance. One specific application is foreshortening correction of objects coplanar with the reference spheres. Remaining errors are mainly due to incorrect landmark definition. In our setup, these were exaggerated by the visual/manual image-evaluation process. Automated image analysis has been shown for similar tasks to minimize these errors considerably.

Keywords Dental radiography · Digital · Measurement · Accuracy · Projection geometry

F. Roeder · D. Brüllmann · B. d'Hoedt · R. Schulze
Department of Oral Surgery (and Oral Radiology),
University Medical Center of the Johannes-Gutenberg-University Mainz, Dental School,
Augustusplatz 2,
55131 Mainz, Germany

F. Roeder (✉)
Poliklinik für Zahnärztliche Chirurgie,
Universitätsmedizin der Johannes-Gutenberg-Universität Mainz,
Augustusplatz 2,
55131 Mainz, Germany
e-mail: roederfe@uni-mainz.de

Introduction

A major problem in (dental) radiography is the appearance of distortions of the 3D object of interest in the 2D projection [1, 2]. They occur if the object's main axis is not parallel to the receptor plane and the central beam of the X-rays is not perpendicular to that plane. Both requirements should be fulfilled in "paralleling technique"; however, in reality, these prerequisites are hard and sometimes even impossible to achieve [2]. The anatomy, particularly in the upper jaw, complicates the ideal positioning of the receptor. This results in an angle between tooth and respective receptor axis differing from the optimum, i.e., a parallel orientation, by an estimated angle varying between 10° and 40°. The projective transformation applied to an object being radiographed essentially is a many-to-one mapping process. The consequence is a distorted and foreshortened image of the object (here tooth). This loss of information yields inaccuracies in diagnostic evaluation. The object is mapped in reduced size as a function of the angulation between the object's main axis and the receptor plane. On the other hand, the knowledge of object sizes and distances, however, is an essential condition for many diagnostic tasks. For example, the exact tooth (root) length is important for an endodontic or prosthodontic therapy. The amount of marginal bone loss is essential for the initiation of a parodontal treatment. Even if compromised due to the 2D nature of a radiographic projection image, for an approximative calculation of the bone loss, the tooth length can be used as reference [3, 4]. In general, such measurements tend to underestimate the true bone loss [5, 6]. Also, errors occur in working length determination during an endodontic treatment [7]. Without any technique to correct distortions resulting from angulations of imaged objects, there will be a nonreproducible projection geometry. That is because the exact position of the receptor in relation to the object of interest is not reproducible [8]. Therefore, in dentistry, many approaches have been developed to standardize projection geometry, i.e., the spatial relation between focal spot, receptor, and object of interest [9, 10]. For instance, to eliminate the errors in the projection of the tooth size, individual filmholders and aiming devices were developed [5, 11, 12]. But especially in the upper jaw, an inclination between a tooth's main axis and the receptor will not be avoidable [2, 8]. It is impossible to eradicate all inaccuracies which lead to significant errors in length determination in dental radiographs [13]. Otherwise, metal spheres are often used as reference objects to adjust the magnification error in dental radiographs by the rule of proportion, particularly in dental implantology [14]. We are not aware, however, that they have been used so far to correct for the distortion and angulation of the object of interest.

This study will show that the positioning of three steel spheres around the object (tooth) coplanar to its main axis enables the inference of the actual projection geometry effective during exposition. Details concerning the a posteriori computation of the projection geometry from three noncollinear reference spheres have been described [15]. In this work, we introduce the particular application of the technique to correct for (e.g., vertical) angular disparity and, therefore, the distortion, as much as the magnification, of the imaged object. It is possible to calculate the length of an object with high accuracy, which we show here using ex vivo objects (teeth). An earlier test with an optimized testing device made of thin steel wire (5 mm length) located coplanar to the center points of three surrounding steel spheres (diameters 2.00 and 3.00 mm) revealed a mean relative length error ranging between 0.4% (for the 3.00-mm sphere diameter) and 0.6% (for the 2.00-mm sphere diameter) [15].

Now, a more realistic setup with human anatomic structures and a more difficult landmark detection of the object's endpoints and the elliptical axis of the imaged sphere in the projection is created. The aim of this study was to determine the capability of the method to correct for distortion errors in an ex vivo setup.

We expect an increasing error in comparison to the former in vitro testing device. Above that, we assume that the error in length measurement will grow with decreasing sphere diameter and increasing angulation of the investigated tooth.

Materials and methods

Theory

The following situation is considered in a 3D Cartesian coordinate system. Let the 3D coordinates be represented without apostrophe, whereas all coordinates lying within the y–z image plane (Fig. 1) are denoted by an apostrophe. The "reference sphere method" (RSM) determines the depth coordinates of the center of the reference spheres placed in the object plane from the elliptical distortion of their shadows (Fig. 1) [15, 16]. The main axis of the elliptically distorted sphere image $\overline{(R'S')}$ has to be identified in order to infer the 3D position of each sphere's center point. From these calculations, we obtain three points in space (i.e., the three center points of the reference spheres=$M_t(x_t, y_t, z_t)$ with $t \in \{1, 2, 3\}$). Since three points, if not located in one line, define a plane, we obtain the "reference sphere plane" (RSP) from [17]:

$$Ax + By + Cz + D = 0. \tag{1}$$

(The coefficients A, B, C, and D determine the relation of the plane to the x-, y-, and z-axis as well as to the point of origin.)

This plane is parameterized by the determinant [17]:

$$\begin{vmatrix} x - x_1 & y - y_1 & z - z_1 \\ x_2 - x_1 & y_2 - y_1 & z_2 - z_1 \\ x_3 - x_1 & y_3 - y_1 & z_3 - z_1 \end{vmatrix}. \tag{2}$$

Each object point forms a straight line (the projection line) with its corresponding image point. All projection lines necessarily intersect in the source point $F(x_F, 0, 0)$ (Fig. 1). By means of two object (tooth) landmark points (crown tip and root tip), it is possible to calculate the intersections $S(x_S, y_S, z_S)$ of these projection lines with the RSP by [17]:

$$x_S = -\frac{Be + Cf + D}{A + Bk + Ch}$$
$$y_S = kx_S + e$$
$$z_S = hx_S + f$$

where $e = y_{P'}$, $f = z_{P'}$, $h = -\frac{z_{P'}}{x_F}$, and $k = \frac{z_{P'}}{x_F}$ with x_F=depth coordinate of the source point, $y_{P'} = y -$ coordinate of the

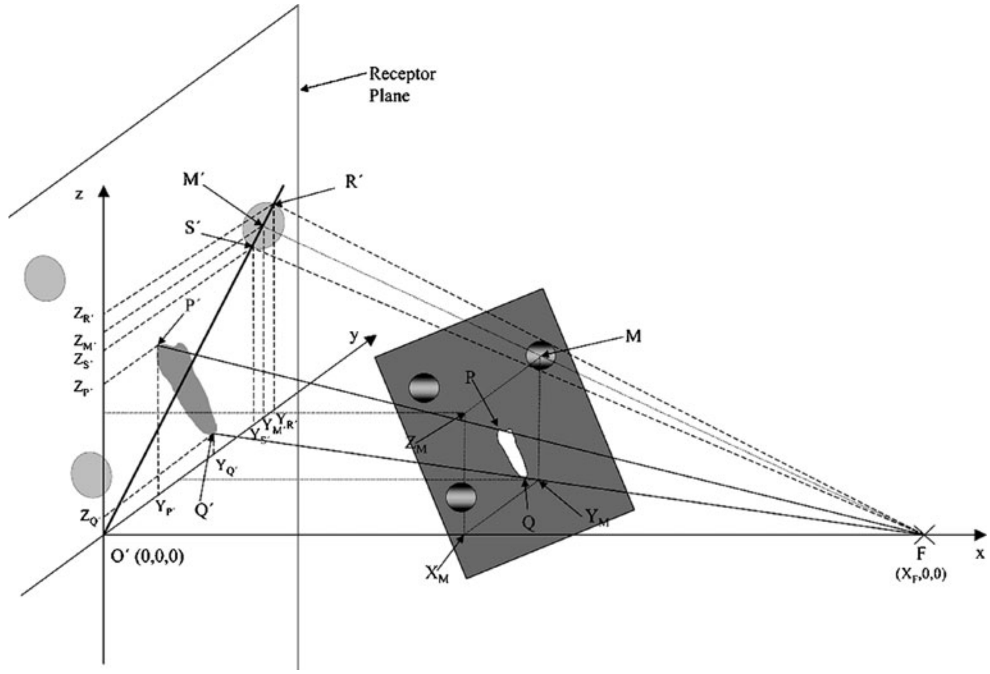

Fig. 1 Projection geometry with a tooth coplanar to a triplet of reference spheres. The shadows of these spheres are used to determine the entire geometry under the assumption that the source-to-receptor distance x_F is known. From this information, any dimension within the reference plane may be corrected by the algorithm for foreshortening and magnification. *M* 3D sphere center point, *PQ* distance under examination, *R'S'* 2D distance determining the elliptical distortion of the shadow. All 2D image coordinate points are marked with an *apostrophe*

projected crown tip, and $z_{P'} = z-$coordinate of the projected crown tip to calculate the coordinates of *P* (crown tip). For *Q* (root tip), the calculation is analogical (for the illustration, see Fig. 1).

The latter process is nothing else than backprojecting the image onto the plane which describes best the original orientation and location of the object. Thereby, distorted distances in the image become rescaled to their original size (Fig. 1). Consequently, the distance between the object endpoints $P(x_P, y_P, z_P)$ and $Q(x_Q, y_Q, z_Q)$ which corresponds to the object (tooth) length *d* (Fig. 1) is finally obtained from [17]:

$$d = \sqrt{\left(x_Q - x_P\right)^2 + \left(y_Q - y_P\right)^2 + \left(z_Q - z_P\right)^2}. \qquad (3)$$

RSM is capable of determining the projection geometry of the 3D anatomic scenery from one 2D image. That means that the 6 degrees of freedom of an object in space are defined [15]. A correction of the angulation of the object axis in relation to the receptor, the true object length, and the magnification of the mapped object can be calculated. It is interesting to note that, for an unknown source-to-receptor distance (x_F), the projection geometry is also determined, however relatively up to the scaling factor $\frac{x_F}{x_F - x_P}$ for *P* or $\frac{x_F}{x_F - x_Q}$ for *Q*, respectively.

Experimental evaluation

Two segments (one permanent canine in the right mandible [length 20.90 mm] and one permanent first molar in the left mandible [length 19.65 mm]) of dry human mandibles, providing exemplarily one single-rooted and one multi-rooted tooth, were available. We thought that examining a higher amount of teeth would not have a significant effect on the results presented here. The teeth were exposed at eight different angulations (0°, 7°, 10°, 20°, 25°, 30°, 35°, and 40°) relative to the charge-coupled device (CCD) receptor to find out which effect the growing angulation has on the error in length determination. Five different typical exposure times (0.04, 0.05, 0.06, 0.08, and 0.10 s) for intraoral X-ray radiographs were selected. In a former study, the effect of the exposure time on the calculation of the sphere center coordinates has been shown [15]. An increasing exposure time produces a decreasing size of the projected object. This is due to the increasing overexposure toward its image boundary, resulting in an underestimation of the diameter. We used an experimental setup (optical bench) where the central beam was aiming perpendicular to the center of the CCD receptor, according to right-angle technique (Fig. 2). Both the realistic source-to-receptor distance (254.3 mm) and pixel size (0.0195 mm) of a commercial dental CCD receptor (Full Size Sensor, Sirona Dental Systems GmbH, Bensheim, Germany) were known. The radiographs were taken with an X-ray apparatus using 60-kV tube voltage and 7-mA heat current (Heliodent DS, Sirona Dental Systems GmbH, Bensheim, Germany). Altogether, 95 radiographs (Fig. 3) were evaluated.

Exemplarily, we chose the assessment of tooth length because a tooth is a solid object which can be examined and measured precisely after extraction. We believe it is possible to evaluate the exactness of this method more accurately, rather than examining, e.g., alveolar bone loss or bony defects, respectively. Our hypothesis, based on

Fig. 2 Experimental setup on an optical bench. Here, the dry mandible segment with a lower molar equipped with the three reference spheres is exposed in a vertical angle of roughly 25° relative to the receptor plane (commercial CCD receptor)

geometry, is that the evaluation of any structure or defect should be more accurate than using the common technique to merely correct magnification (rule of proportion) [14, 18, 20].

Three steel spheres were attached roughly coplanar with the tooth's main axis using dental wax. The sphere diameters of d_1=2.00 mm and d_2=3.00 mm were selected as we had observed acceptable accuracy for these diameters in a prior study [15]. They also guaranteed acceptable handling when attaching the spheres to the object of interest in the narrow oral cavity. The average vertical inclination of the object's main axis relative to the receptor plane was 24.4° for d_1 (eight different positions, 40 exposures) and 22.6° for d_2 (11 different positions, 55 exposures) as measured by a protractor. In an image-editing software (Adobe Photoshop 7.0, Adobe Systems Inc., Mountain View, USA), the length, as defined from crown to root tip (Fig. 4), was assessed manually by one observer (F.R.) with a mouse-driven cursor once for every image (five times for every adjustment by having five exposure times of every projection geometry). The measurement was made under standardized viewing conditions in a darkened room. The required coordinates and distances in the reference sphere shadows were measured accordingly; the exact evaluation process has already been described in detail [15]. The data was fed into the RSM algorithm implemented in a spreadsheet software (Microsoft Excel 2000, Microsoft Corporation, Richmond, USA) and transferred to a scientific statistical software program for descriptive analysis (SPSS Statistics 17.0, SPSS, Chicago, IL, USA). Different groups were compared using the Wilcoxon rank-sum test. A p value ≤0.05 was considered statistically significant. True tooth length (d_{truth}), assessed with a caliper after extraction of the respective tooth, was compared to the results of RSM (d_{RSM}) and to a conventional method (C) (d_{C}), which simply applied the rule of proportion $\left(\text{object size}_{\mathrm{real}} = \text{object size}_{\mathrm{image}} \times \text{sphere diameter}_{\mathrm{real}}/\text{sphere diameter}_{\mathrm{image}}\right)$ based on the mean magnification of the three reference spheres. For comparison, absolute ($d_{\mathrm{RSM/C}}-d_{\mathrm{truth}}$) and relative $\left(\left(d_{\mathrm{RSM/C}} - d_{\mathrm{truth}}\right) \times 100/d_{\mathrm{truth}}\right)$ errors were considered.

Results

The method to calculate tooth length introduced here (RSM) has a higher grade of accuracy when using three reference spheres with a larger diameter (d_2=3.00 mm) than using smaller ones (d_1=2.00 mm). A correlation between the size of the error and the inclination of the tooth axis relative to the receptor can be detected. By increasing the angulation between the tooth's main axis and the receptor

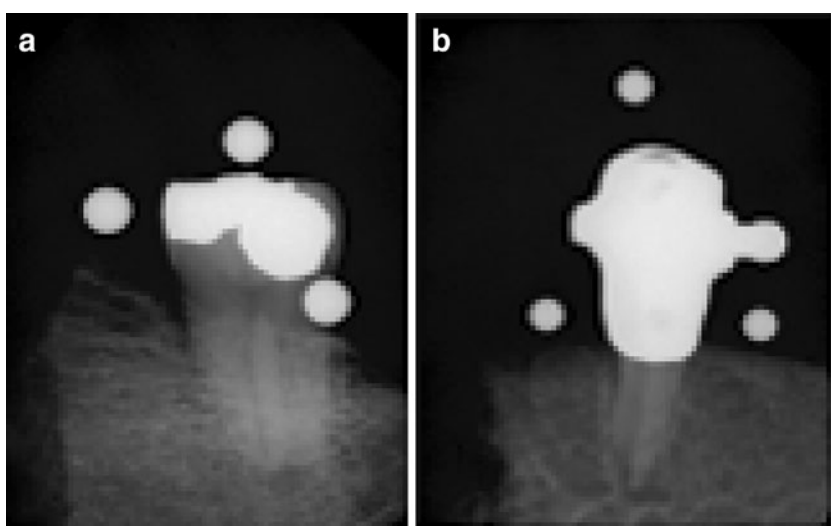

Fig. 3 Radiographs of **a** lower first permanent left molar in a dry human mandible section with 3.00-mm-diameter spheres and **b** lower permanent right canine in a dry human mandible section with 2.00-mm-diameter spheres

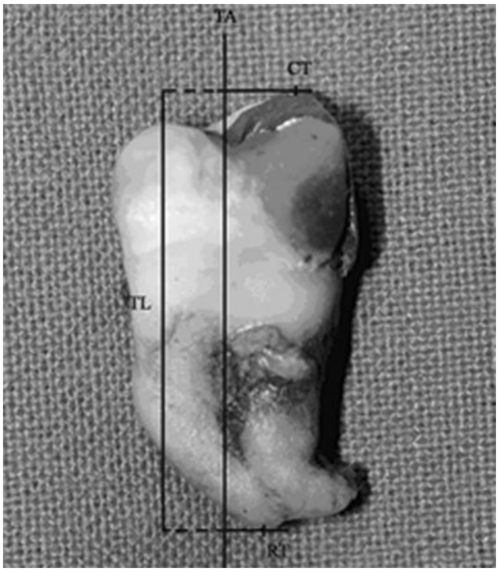

Fig. 4 Tooth length (*TL*) defined as the distance between the highest crown tip point (*CT*) and the lowest root tip point (*RT*) projected perpendicular to the tooth length axis (*TA*) which is intersecting the middle of the occlusal surface and the middle of the bifurcation or trifurcation (multirooted teeth) or intersecting the middle of incisal ridge and the root tip (single-rooted teeth)

plane, the assessed object length shows a growing overestimation of the true length. So the error increases with growing angulation between object and receptor and decreasing sphere diameter (Table 1). For an angulation up to 30°, the relative length error remains lower than 5% for both sphere sizes (Fig. 5).

For both methods (RSM and C), length errors were significantly ($p<0.0001$) correlated with the inclination relative to the receptor plane and to the sphere diameter (Fig. 5) but not to the various exposure times. The errors were not significantly correlated to the evaluation of a single-rooted or multirooted tooth for both methods. The conventional method underestimates whereas RSM slightly overestimates the true object size with increasing inclination. The tooth length calculated with the conventional method (C) was less accurate and reveals a permanent underestimation of the true object size (Table 1).

The mean relative length error ± standard deviation (SD) using RSM was 2.28±5.50% (absolute=0.44±1.10 mm) for d_1 and 0.46±4.27% (absolute=0.09±0.87 mm) for d_2. For C, it was −13.58±11.72% (absolute=−2.61±2.26 mm) for d_1 and −9.90±7.66% (absolute=−1.94±1.50 mm) for d_2. For detailed statistics, see Table 1.

Discussion

RSM allows for complete a posteriori determination of the imaging geometry under the assumption of a known source-to-receptor distance. The general methodology has been described in detail elsewhere [15]. One specific application is foreshortening correction of objects (e.g., teeth) coplanar with the three reference spheres that, as per mathematical definition, span a plane if not located in one line. Our experiments reveal a higher accuracy in radiographic length measurement when using RSM compared to the prevalent conventional estimation method that is based on the rule of proportion (C). This is particularly true when the object's main axis features an inclination relative to the receptor plane, appearing most notably in the upper jaw. It should be noted here that we are not aware of other methods of 3D projection image evaluation considering this factor a posteriori. Commonly, a priori optimization of the imaging geometry to avoid alignment errors is aimed for, e.g., by means of more or less complicated individualized devices [11, 12]. Even then, however, parallelism between tooth and receptor is often hard to achieve. Our a posteriori correction method requires application of three small reference spheres, yet no assumption on the actual orientation between object and image detector is made.

Our results indicate a relatively low accuracy of RSM when a manual image-evaluation process is applied. Also, with increasing angulations, the definition of the object

Table 1 Descriptive statistic of the relative (in percent) and absolute (in millimeters) length error in tooth length determination of the RSM versus the conventional method (rule of proportion) for two different sphere diameters

	Reference sphere diameter 2.00mm				Reference sphere diameter 3.00mm			
	RSM		Conventional		RSM		Conventional	
	Relative (%)	Absolute (mm)	Relative (%)	Absolute (mm)	Relative (%)	Absolute (mm)	Relative (%)	Absolute (mm)
Mean ± SD	2.28±5.50	0.44±1.10	−13.58±11.72	−2.61±2.26	0.46±4.27	0.09±0.87	−9.90±7.66	−1.94±1.50
Median	1.19	0.23	−9.44	−1.81	−1.41	−0.28	−7.08	−1.39
95%CI	−2.08–7.37	−0.57–1.46	−36.55–9.39	−7.02–1.80	−3.49–4.41	−0.72–0.89	−24.91–5.11	−4.88–1.00

SD standard deviation of the mean, *95%CI* 95% confidence interval of the mean

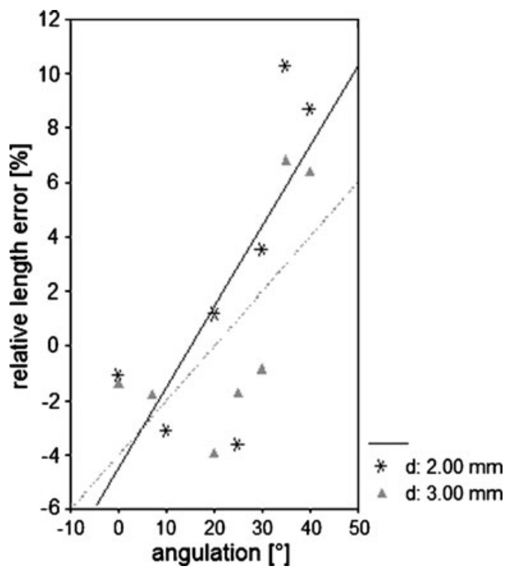

Fig. 5 Relative length error for RSM in dependence of the angulation of the tooth's main axis in relation to the receptor for the sphere diameters (*d*) 2.00 and 3.00 mm. The *straight lines* are calculated by linear regression analysis

(tooth) landmark points becomes more and more difficult, explaining the increasing error for larger angles. Landmark point definition is easier when well-defined objects such as a piece of steel wire are used (Fig. 5) [11, 15]. The increasing error appearing with decreasing sphere diameter is correlated to the accuracy of affecting the 3D position of the reference sphere center in relation to the sphere diameter [15]. The permanent underestimation of the object size by C is due to the decreasing size of the projected tooth with increasing angulation of its main axis relative to the receptor plane. It should also be noted that the conventional method is based on the mean magnification of three spheres as determined along the identical elliptical axis $\overline{R'S'}$. Hence, the conventional method presented here should perform substantially better than any method applied in a clinical situation.

The detection of the exact reference sphere points and anatomic landmark points might be more difficult in an in vivo application because of the scattering induced by the soft tissue [15]. Hence, a slightly increasing error may result in a true in vivo situation. We expect a slight decrease in accuracy in calculating the object size in vivo.

Another source of error is the freehand placement of the reference spheres roughly coplanar to the tooth axis under investigation, yet without knowing the exact 3D shape of the root. The angle φ between the true RSP and the calculated RSP_1 can be mathematically determined by [17]:

$$\varphi = \arccos\left[\frac{AA_1 + BB_1 + CC_1}{\sqrt{(A^2+B^2+C^2)\left(A_1^2+B_1^2+C_1^2\right)}}\right]. \qquad (4)$$

As expected, in comparison to the results of the length evaluation using the testing device (steel wire), the results in this study are less accurate [15]. However, for d_2, the discrepancy of the relative mean error is small (difference ~0.1%). For a clinical application, spheres of 3.00 mm in diameter seem to provide acceptable results, even for angulations as much as 30° (relative length error <5%). For an automated evaluation using sophisticated and task-specific optimization methods, as described in a previously published study [15], we expect that the diameter could be further reduced.

This brings us to the question on how the method may be used in a clinical situation. One idea is to use prefabricated small plastic devices containing the three spheres, which can be attached to an object of interest during exposition. The device would have to be small enough to be imaged completely on one intraoral radiograph. If the triangle spanned by the spheres was accurately known from the fabrication process, this additional information could be used to further reduce errors. We already have developed the mathematics necessary for this special case. By using intraoral radiographs with one metal sphere in an edentulous area for the preoperative selection of dental implant size for a solitary tooth replacement, the measurement errors caused by vertical and horizontal distortion are not considered [18–20]. Compared to this technique (i.e., the conventional method), particularly in the upper jaw, the use of RSM could determine the vertical bone height and the horizontal space width (when the image is taken orthoradially) with a higher accuracy. A similar indication could be the preoperative diagnosis in case of immediate implantation of an enossal implant. The depth and width of the alveolus and distances to important anatomic structures (inferior alveolar nerve, maxillary sinus) could be measured by correcting distortion and magnification. RSM could help to choose the optimal dimension of the implant with a single intraoral radiograph. Also, the dimension of any structure, for example, pathologic processes such as intrabony cysts and tumors, lying in the RSP, can be calculated accordingly. Likewise, this method could increase the accuracy by monitoring the process of marginal bone loss or intrabony defects with intraoral radiographs, mainly when the tooth length is used as reference distance [3, 4]. No additional equipment, like aiming devices or individual filmholders [5, 11, 12], is necessary to standardize projection geometry because it can be assessed with RSM. Probably, the well-known underestimation of alveolar bone loss [3, 5, 6] is partly due to a noncorrected distortion of the examined part of the jaw. Our suggestion could be supported by the observation that this effect appears more commonly in the upper jaw [3, 21]. Other possible options for clinical use have been already specified [15]. RSM for few-view 3D reconstruction purposes has been extensively discussed before [22].

In conclusion, RSM also yields considerable errors for the specific application of tooth length assessments, which are mainly due to inaccuracies in the manual image-evaluation process. It does, however, perform significantly better than the best possible results based on conventional magnification-related correction (C). Automated image analysis will presumably help to minimize errors considerably. A software for the detection of the sphere shadow has already been developed [23]. Another software tool, using the algorithm introduced here for length correction, where only the anatomical landmarks have to be identified by the user, is under progress. The main application for RSM, i.e., providing an image registration tool for 3D reconstruction from 2D radiographic views, is currently being further developed [22]. Foreshortening correction, using RSM, may be another future application, particularly for large-size medical radiographs [24–33].

Conflict of interest The authors declare that they have no conflict of interest.

References

1. Van Aken J (1969) Optimum conditions for intraoral roentgenograms. Oral Surg 27:475–491
2. Schulze R, d'Hoedt B (2002) A method to calculate angular disparities between object and receptor in "paralleling technique". Dentomaxillofac Radiol 31:32–38
3. Kim TS, Obst C, Zehaczek S, Geenen C (2008) Detection of bone loss with different X-ray techniques in periodontal patients. J Periodontol 79:1141–1149
4. Steffensen B, Suzuki H, Caffesse RG, Ash MM (1987) Repair of periodontal angular bony defects evaluated by one- and two-dimensional radiographic analysis. Oral Surg Oral Med Oral Pathol Oral Radiol Endod 63:109–114
5. Benn DK (1990) A review of the reliability of radiographic measurements in estimating alveolar bone changes. J Clin Periodontol 17:14–21
6. Eickholz P, Riess T, Lenhard M, Haßfeld S, Staehle HJ (1999) Digital radiography of interproximal bone loss. J Clin Periodontol 26:294–300
7. Williams CB, Joyce AP, Roberts S (2006) A comparison between in vivo radiographic working length determination and measurement after extraction. J Endod 32:624–627
8. Schulze R, d'Hoedt B (2001) Mathematical analysis of projection errors in "paralleling technique" with respect to implant geometry. Clin Oral Implants Res 12:364–371
9. Payne AGT, Solomons YF, Lowine JF (1999) Standardization of radiographs for mandibular implant-supported overdentures: review and innovation. Clin Oral Implants Res 10:307–319
10. Dixon CA, Hildebolt CF (2005) An overview of radiographic film holders. Dentmaxillofac Radiol 34:67–73
11. Dubrez B, Jacot-Dsecombes S, Cimasoni G (1995) Reliability of a paralleling instrument for dental radiographs. Oral Surg Oral Med Oral Pathol Oral Radiol Endod 80:358–364
12. Zappa U, Simona C, Graf H, van Aken J (1991) In vivo determination of radiographic projection errors produced by a novel filmholder and an x-ray beam manipulator. J Periodontol 62:674–683
13. Eickholz P, Hausmann E (2000) Accuracy of radiographic assessment of interproximal bone loss in intrabony defects using linear measurements. Eur J Oral Sci 108:70–73
14. Behneke N, Tetsch P (1985) Diagnostik und Planung von Implantaten im zahnlosen Unterkiefer. Fortsch Zahnärztl Implantol 1:266–271
15. Schulze R, Bruellmann DD, Roeder F, d'Hoedt B (2004) Determination of projection geometry from quantitative assessment of the distortion of spherical references in single-view projection radiography. Med Phys 31:2849–2854
16. Hilbert D, Cohn-Vossen S (1999) The cylinder, the cone, the conic sections and their surfaces of revolution. In: Geometry and the imagination, 2nd edn. Chelsea Publishing Company, New York, pp 7–9
17. Bronstein IN, Semendjajew KA, Musiol G, Mühlig H (2000) Analytische Geometrie des Raumes. In: Taschenbuch der Mathematik, 5th edn. Verlag Harri Deutsch, Thun und Frankfurt am Main, pp 220–226
18. Schropp L, Stavropoulos A, Gotfredsen E, Wenzal A (2009) Calibration of radiographs by a reference metal ball affects preoperative selection of implant size. Clin Oral Invest (in press)
19. Tyndall AA, Brooks SL (2000) Selection criteria for dental implant site imaging: a position paper of the American Academy of Oral and Maxillofacial Radiology. Oral Surg Oral Med Oral Pathol Oral Radiol Endod 89:630–637
20. BouSerhal C, Jacobs R, Quirynen M, van Steenberghe D (2002) Imaging technique selection for the preoperative planning of oral implants: a review of the literature. Clin Implant Dent Relat Res 4:156–172
21. Volchansky A, Cleaton-Jones P, Drummond S, Bönecker M (2006) Technique for linear measurement on panoramic and periapical radiographs: a pilot study. Quintessence Int 37:191–197
22. Schulze R, Heil U, Weinheimer O, Gross D, Bruellmann DD, Thomas E, Schwanecke U, Schoemer E (2008) Accurate registration of random radiographic projections based on three spherical references for the purpose of few-view 3D reconstruction. Med Phys 35:546–555
23. Schulze R, Weinheimer O, Bruellmann DD, Roeder F, d'Hoedt B, Schoemer E (2005) Software for automated application of a reference-based method for a posteriori determination of the effective radiographic image geometry. Dentmaxillofac Radiol 34:205–211
24. Weijers RE, Kessels AG, Walenkamp GH, van Mameren H, Kemerink GJ (2005) Effect of tube angulation on the measurement of intermetatarsal angles. J Am Podiatr Med Assoc 95:370–375
25. Weijers R, Kemerink G, van Mameren H, Walenkamp G, Kessels AG (2005) The intermetatarsal and metatarsal declination angles: geometry as a source of error. Foot Ankle Int 26:387–393
26. Camasta CA, Pontious J, Boyd RB (1991) Quantifying magnification in pedal radiographs. J Am Podiatr Med Assoc 81:545–548
27. Cheng AC, Lew KK, Bhole S (1997) Head positioning and projection errors in submentovertex radiographic analysis. Singapore Dent J 22:13–17
28. Malkoc S, Sari Z, Usumez S, Koyuturk AE (2005) The effect of head rotation on cephalometric radiographs. Eur J Orthod 27:315–321
29. Yoon YJ, Kim KS, Hwang MS, Kim HJ, Choi EH, Kim KW (2001) Effect of head rotation on lateral cephalometric radiographs. Angle Orthod 71:396–403
30. Yoon YJ, Kim DH, Yu PS, Kim HJ, Choi EH, Kim KW (2002) Effect of head rotation on posteroanterior cephalometric radiographs. Angle Orthod 72:36–42
31. Frobin W, Brinckmann P, Leivseth G, Biggemann M, Reikeras O (1996) Precision measurement of segmental motion from flexion–extension radiographs of the lumbar spine. Clin Biomech 11:457–465
32. Leivseth G, Kolstad F, Nygaard OP, Zoega B, Frobin W, Brinckmann P (2006) Comparing precision of distortion-compensated and stereophotogrammetric roentgen analysis when monitoring fusion in the cervical spine. Eur Spine J 15:774–779
33. Owens EF Jr (1992) Line drawing analysis of static cervical X ray used in chiropractic. J Manipulative Physiol Ther 15:442–449